Evolution of normal stress and surface roughness in buckled thin films

Palasantzas, G.; De Hosson, J. Th. M.

Published in:
Journal of Applied Physics

DOI:
10.1063/1.1528299

Evolution of normal stress and surface roughness in buckled thin films

G. Palasantzas and J. Th. M. De Hosson[a)]
Department of Applied Physics, Materials Science Center and Netherlands Institute for Metals Research, University of Groningen, Nijenborgh 4, 9747 AG Groningen, The Netherlands

(Received 17 July 2002; accepted 22 October 2002)

In this work we investigate buckling of compressed elastic thin films, which are bonded onto a viscous layer of finite thickness. It is found that the normal stress exerted by the viscous layer on the elastic film evolves with time showing a minimum at early buckling stages, while it increases at later stages. The normal stress also shows a minimum as a function of applied compressive stress, which depends strongly on the viscosity of the underlying layer and strain values. Furthermore, with decreasing viscosity the film roughness amplitude also shows a minimum at early buckling stages. The effect of the viscosity becomes more pronounced with increasing strain in the film. Finally, decreasing elastic film thickness and/or increasing viscous layer thickness also enhance buckling roughness. © *2003 American Institute of Physics.* [DOI: 10.1063/1.1528299]

I. INTRODUCTION

Thin films in modern device technology are often in a state of compression. Actually, the mismatch between thermal expansion coefficients may produce compressive stresses in thermal barrier coatings and heteroepitaxial growth may be accompanied by the evolution of compressive stresses. Nevertheless, by adhering a compressed thin film to a low viscosity glass, the compressive stresses can be relieved. In particular, this methodology has been explored in the growth of low dislocation and relaxed heteroepitaxial semiconductor films.[1] Moreover, atomic force microscopy and cross-sectional scanning electron microscopy/transmission electron microscopy have shown buckling of compressively strained SiGe films (deposited on borophosphorosilicate) during annealing.[2]

In general, any freestanding film, which is subject to compression, will spontaneously display buckling at lateral length scales that strongly depend on its elastic properties, the thickness, and the magnitude of the applied stress.[3] The film expands out of its plane, which leads to buckling, with a characteristic wavelength that is the result of the competition of the in-plane strain relaxation and the elastic stress due to bending.[4,5]

So far, a stability analysis of the buckling problem for thin elastic films with a finite thickness onto a viscous layer predicted the growth rates of preexisting undulations that develop in time.[4] However, the former calculations did not encounter the problem of how the buckling amplitude develops assuming an initial rough profile of the elastic film, as well as the how the normal stress that the elastic film feels from the viscous films changes with progressing film buckling. This will be the topic of the present work where for simplicity we will consider the case of the initial elastic film surface roughness to be self-affine type. The latter assumption is based on the fact that the formation of self-affine roughness has been observed for a wide range of deposited thin films (i.e., metallic, semiconductor, and organic).[6–9]

[a)]Author to whom correspondence should be addressed; electronic mail: hossonj@phys.rug.nl

II. BUCKLING FILM THEORY

We consider an elastic film of thickness h_f, Young modulus E, and Poisson ratio ν. The elastic film is assumed to be bonded onto a viscous substrate with viscosity η and thickness h_g, which is also assumed to be bonded onto a rigid substrate (Fig. 1). The elastic film is under compressive stress σ, which is related to a misfit strain ϵ by $\sigma = E\epsilon/(1-\nu)$. When the film has buckled under compression and bending with the vertical displacement $h(\mathbf{r})$ ($\ll h_f$) given by Refs. 3 and 4 for wavelength much larger than fh_f

$$\frac{Eh_f^3}{12(1-\nu^2)}\nabla^4 h + \sigma h_f \nabla^2 h + \sigma_N = 0. \tag{1}$$

In Eq. (1) σ_N is the normal stress exerted on the film by the viscous substrate (at the elastic/viscous film interface), and $\mathbf{r}=(x,y)$ the in-plane position vector. Assuming the Fourier transform $h(\mathbf{r}) = \int h(\mathbf{k},t)e^{-i\mathbf{k}\cdot\mathbf{r}}d^2\mathbf{r}$, Eq. (1) yields the normal stress σ_N

$$\sigma_N = \int \left[\sigma h_f k^2 - \frac{Eh_f^3}{12(1-\nu^2)}k^4 \right] h(\mathbf{k},t)e^{-i\mathbf{k}\cdot\mathbf{r}}d^2\mathbf{k}, \tag{2}$$

with $k^2 = k_x^2 + k_y^2$. The problem of an infinite viscous layer ($h_g \to +\infty$) was solved in the past by Mullins.[5] For the linear boundary value problem the velocity of the elastic film surface $\partial h/\partial t$ is proportional to a strain rate $\sigma_N(k,t)/\eta$ for each Fourier mode $h(k,t)$ of the form[4]

$$\frac{\partial h(k,t)}{\partial t} = g\frac{\sigma_N(k,t)}{2\eta k}, \quad g = \frac{\sinh(2h_g k) - 2h_g k}{1+\cosh(2h_g k) + 2(h_g k)^2}, \tag{3}$$

with $\sigma_N(k,t) = \{\sigma h_f k^2 - [Eh_f^3/12(1-\nu^2)]k^4\} h(k,t)$. Integration of Eq. (3) yields[4]

$$h(k,t) = h(k,0)e^{a(k)t}$$

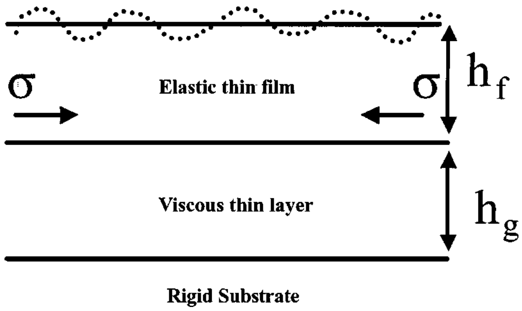

FIG. 1. Schematic of the system elastic film/viscous layer/rigid substrate.

$$a(k)=\frac{E}{24\eta(1-\nu^2)}\left[\frac{\sinh(2h_gk)-2h_gk}{1+\cosh(2h_gk)+2(h_gk)^2}\right]\times[\beta(h_fk)-(h_fk)^3], \quad (4)$$

with $\beta=12\epsilon(1+\nu)$ and ϵ represents the misfit strain.

III. ROUGHNESS MODELS AND RELATED PARAMETERS

In the following we will assume translation invariant film surface roughness or $\langle h(\mathbf{k},t)h(\mathbf{k}',t)\rangle=[(2\pi)^4/A]\times\langle|h(\mathbf{k},t)|^2\rangle\delta^2(\mathbf{k}+\mathbf{k}')$. A is the average macroscopic flat surface area, and $\langle ...\rangle$ means ensemble average over possible roughness configurations. Therefore, since Eq. (4) yields the roughness spectrum $\langle|h(\mathbf{k},t)|^2\rangle$, we can obtain the rms roughness amplitude of the buckled film surface and the average normal stress

$$w(t)=\left[\frac{(2\pi)^5}{A}\int_{0\leq k\leq Q_c}\langle|h(\mathbf{k},0)|^2\rangle e^{2a(k)t}k\,dk\right]^{1/2}, \quad (5)$$

$$\sigma^{\mathrm{av}}{}_N=\left\{\frac{(2\pi)^5}{A}\int_0^{Q_c}\left[\sigma h_f k^2-\frac{Eh_f^3}{12(1-\nu^2)}k^4\right]^2\times\langle|h(\mathbf{k},0)|^2\rangle e^{2a(k)t}k\,dk\right\}^{1/2} \quad (6)$$

under the constraint that $w(t)\ll h_f$ because the present theory requires weak buckling.[4]

Furthermore, in order to calculate the roughness related parameters $w(t)$ and $\sigma^{\mathrm{av}}{}_N$, the knowledge of the initial roughness spectrum $\langle|h(\mathbf{k},0)|^2\rangle$ is necessary in Eqs. (5)–(6). Indeed, a wide variety of surfaces/interfaces in thin films are well described by self-affine fractal scaling[6–9] where $\langle|h(\mathbf{k},0)|^2\rangle$ follows the power law scaling relations $\langle|h(\mathbf{k},0)|^2\rangle\propto k^{-2-2H}$ if $k\xi\gg1$, and $\langle|h(\mathbf{k},0)|^2\rangle\propto$const if $k\xi\ll1$. ξ is the in-plane roughness correlation length of the initial film surface. We also define w_0 as the initial roughness amplitude of the film surface at $t=0$. The roughness exponent H is a measure of the degree of surface irregularity, such that small values of H characterize more irregular surfaces at short roughness wavelengths ($<\xi$). This scaling behavior can be described by the simple Lorentzian model[10]

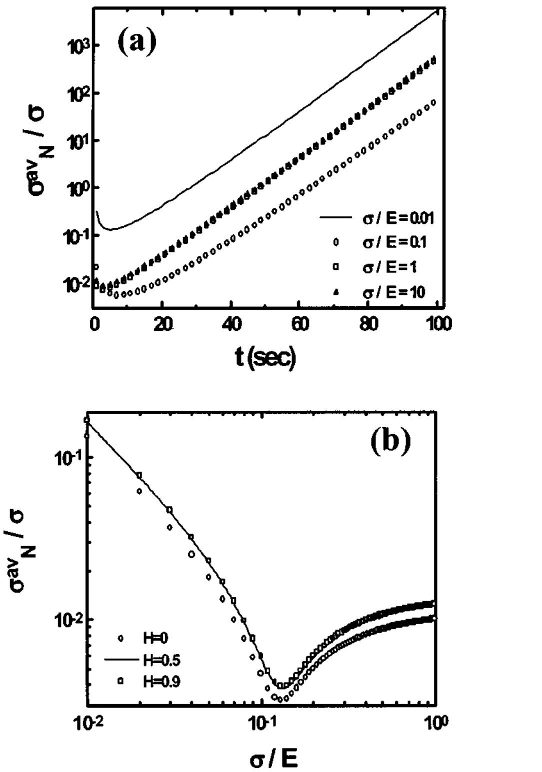

FIG. 2. (a) Average normal stress σ_N^{av} vs evolution time t for viscosity $\eta=1.3\times10^{10}$ Pa s, $H=0.5$, $\epsilon=0.12$, $h_f=30$ nm, $h_g=50$ nm, and various values of the compressive stress σ/E. (b) σ_N^{av} vs σ/E for various roughness exponents H of the initial starting film morphology, $\eta=1.3\times10^{10}$ Pa s, $\epsilon=0.12$, $h_f=30$ nm, and $h_g=50$ nm.

$$\langle|h(\mathbf{k},0)|^2\rangle=\frac{A}{(2\pi)^5}\frac{w_o^2\xi^2}{(1+ak^2\xi^2)^{1+H}}, \quad (7)$$

with $a=(1/2H)[1-(1+aQ_c^2\xi^2)^{-H}]$ if $0<H<1$, and $Q_c=\pi/a_0$ with a_0 on the order of the atomic spacing. It should be realized that Q_c is a rather large number and Eq. (1) breaks down earlier. For other self-affine roughness models see also Ref. 9.

IV. RESULTS AND DISCUSSION

Our calculations were performed for film Young's modulus $E=70$ GPa, Poisson's ratio $v=0.35$, viscosity $\eta=c(1.3\times10^{11}$ Pa s) ($c>0$; variation of the parameter c alters the viscosity), initial rms roughness amplitude $w_0=0.5$ nm ($\ll h_f$), and initial roughness correlation length $\xi=10$ nm. In the following we will investigate the evolution of the normal stress $\sigma^{\mathrm{av}}{}_N$ and the surface roughness amplitude $w(t)$. Finally, we will assume in all cases a constant applied stress, ignoring any stress relaxation at the interfaces which could reduce the applied stress in the film.

Figure 2(a) shows the calculation of σ_N^{av} versus evolution time t for various values of applied compressive stress σ. Indeed, σ_N^{av} initially decreases reaching a minimum, and further increases and becomes larger than the applied stress σ. This can be understood from Eq. (6) if it is written as

$$\sigma_N^{\mathrm{av}} = \left\{ \begin{array}{l} \dfrac{(2\pi)^5}{A}\displaystyle\int_0^{h_f^{-1}\sqrt{\beta}} \left[\sigma h_f k^2 - \dfrac{E h_f^3}{12(1-\nu^2)} k^4 \right]^2 \langle |h(\mathbf{k},0)|^2 \rangle e^{2a(k)t} k\, dk \\ + \dfrac{(2\pi)^5}{A}\displaystyle\int_{h_f^{-1}\sqrt{\beta}}^{Q_c} \left[\sigma h_f k^2 - \dfrac{E h_f^3}{12(1-\nu^2)} k^4 \right]^2 \langle |h(\mathbf{k},0)|^2 \rangle e^{2a(k)t} k\, dk \end{array} \right\}^{1/2} \tag{8}$$

with the first integral incorporating the contribution of unstable wave vectors such that $k < h_f^{-1}\sqrt{\beta}$ or equivalently $a(k) > 0$ which makes the film unstable to buckling. Moreover, the initial film morphology appears to have a moderate impact on σ_N^{av} [Fig. 2(b)], where it is more pronounced for small roughness exponents $H(<0.5)$. As Fig. 2(b) indicates, the magnitude of the normal stress σ_N^{av} will be lower for a rougher initial film morphology (lower roughness exponents H and/or smaller correlation length which leads to larger roughness ratio w_0/ξ for w_0 fixed).

Furthermore, as Figs. 2(b) and 3(a) indicate, with increasing applied compressive stress σ the normal stress σ_N^{av} decreases up to minimum which is shifted for later buckling times ($t \gg g1$) toward lower values of $\sigma(\sim 0.1E)$, while σ_N^{av} increases and reaches saturation for $\sigma > E$. The minimum of σ_N^{av} as a function of σ/E becomes rather sharp as the viscosity η of the layer underneath the buckled film decreases [Fig. 3(b)]. Notably with decreasing misfit strain ϵ, the normal stress σ_N^{av} decreases in magnitude, as well as its minimum shifts to lower values of σ/E [Fig. 3(c)]. In addition with increasing elastic film thickness, the normal stress σ_N^{av} decreases in magnitude with the minimum position being shifted to larger values of the ratio σ/E as Fig. 4(a) indicates. This is due to the fact that the range of unstable wave vectors ($k < h_f^{-1}\sqrt{\beta}$) in Eq. (8) becomes larger. However, the oppo-

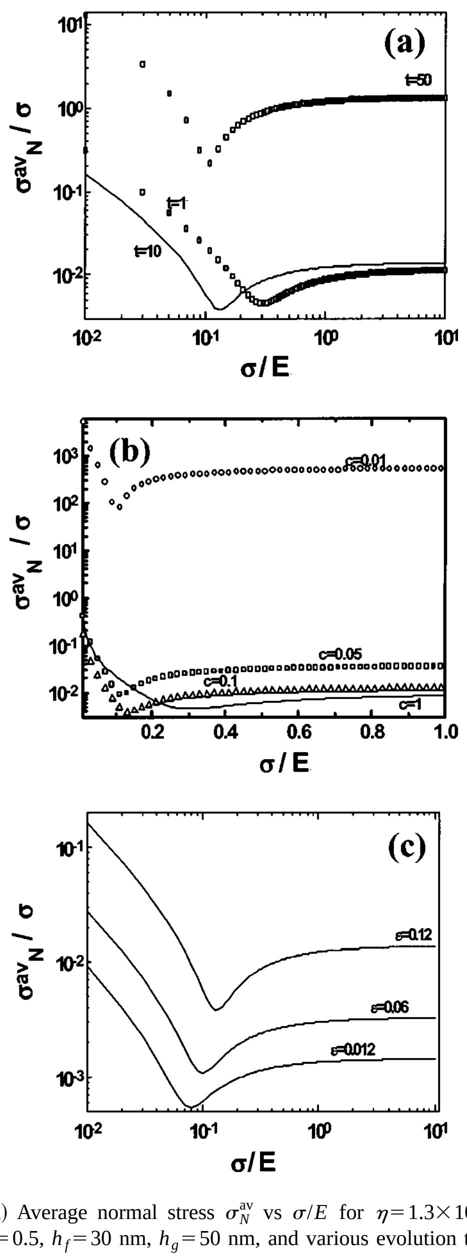

FIG. 3. (a) Average normal stress σ_N^{av} vs σ/E for $\eta = 1.3\times 10^{10}$ Pa s, $\epsilon = 0.12$, $H = 0.5$, $h_f = 30$ nm, $h_g = 50$ nm, and various evolution times t. (b) σ_N^{av} vs σ/E for $t = 10$ s, $\epsilon = 0.12$, $H = 0.5$, $h_f = 30$ nm, $h_g = 50$ nm, and various viscosities $\eta = c(1.3\times 10^{11})$ Pa s. (c) σ_N^{av} vs σ/E for $n = 1.3\times 10^{10}$ Pa s, $t = 10$ s, $H = 0.5$, $h_f = 30$ nm, $h_g = 50$ nm, and various strains ϵ.

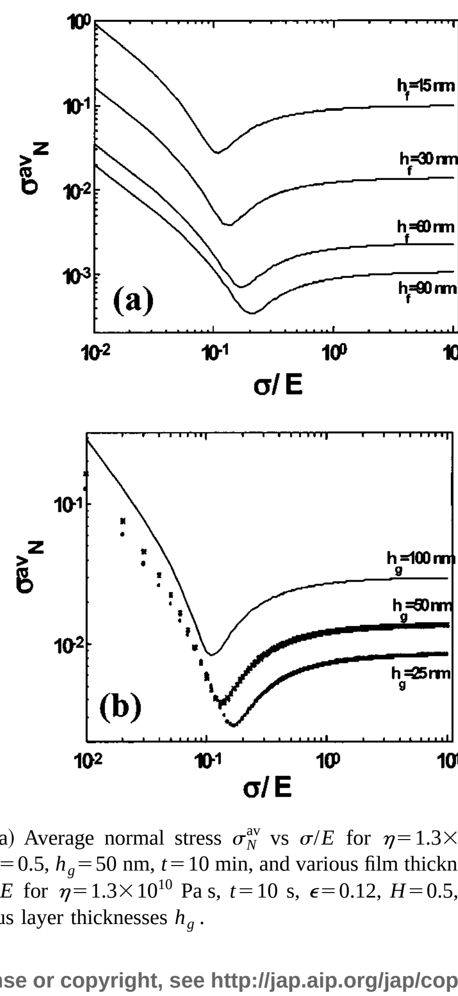

FIG. 4. (a) Average normal stress σ_N^{av} vs σ/E for $\eta = 1.3\times 10^{10}$ Pa s, $\epsilon = 0.12$, $H = 0.5$, $h_g = 50$ nm, $t = 10$ min, and various film thicknesses h_f. (b) σ_N^{av} vs σ/E for $\eta = 1.3\times 10^{10}$ Pa s, $t = 10$ s, $\epsilon = 0.12$, $H = 0.5$, $h_f = 30$ nm, and various layer thicknesses h_g.

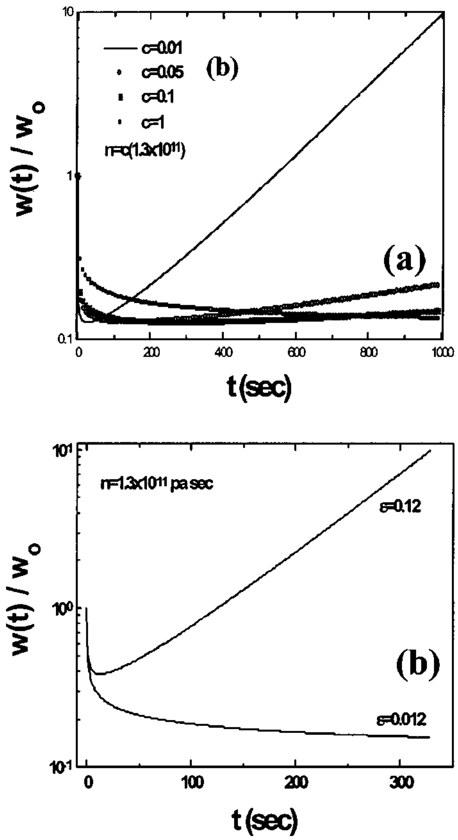

FIG. 5. (a) Amplitude ratio $w(t)/w_0$ vs evolution time t for various viscosities n, $\epsilon=0.012$, $H=0.5$, $h_f=30$ nm, and $h_g=50$ nm. (b) $w(t)/w_0$ vs evolution time t for various strains ϵ, $\eta=1.3\times10^{10}$ Pa s, $H=0.5$, $h_f=30$ nm, $h_g=50$ nm.

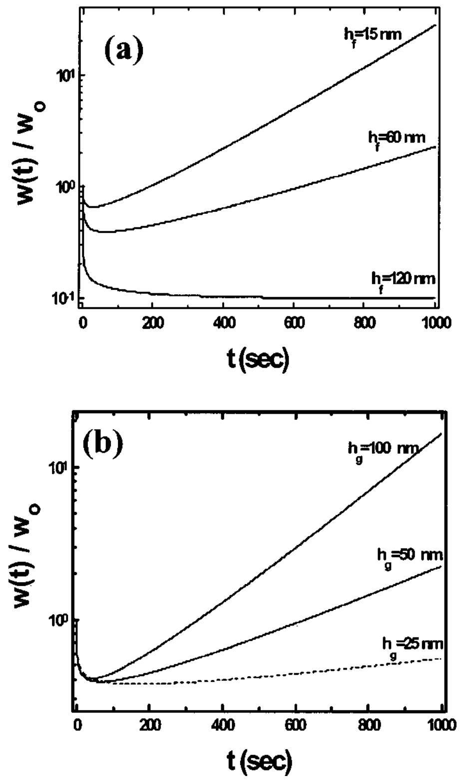

FIG. 6. (a) Amplitude ratio $w(t)/w_0$ vs evolution time t for various film thickness h_f, $\epsilon=0.12$, $H=0.5$, and $h_g=50$ nm. (b) $w(t)/w_0$ vs evolution time t for various thickness h_g, $\eta=1.3\times10^{10}$Pa s, $H=0.5$, $h_g=50$ nm, and $\epsilon=0.12$.

site behavior is observed for σ_N^{av} as the thickness of the viscous layer increases [Fig. 4(b)].

The calculations indicate that the norma1 stress exerted by the viscous layer on the buckled film depends strongly on the film characteristic, which influence its time evolution during buckling. Such behavior of the normal average stress will also have strong implications on characteristic buckling roughness parameters (i.e., roughness amplitude w) as will be shown in the following paragraphs.

Figure 5(a) shows calculations of the rms roughness amplitude $w(t)$ versus time t for various viscosities of the underlying viscous film (see Fig. 1). In all cases we have $w(t)\ll h_f$ so that the linear theory is applicable. With decreasing viscosity η, $w(t)$ decreases for short time scales (stable regime), and increases for later times by becoming larger than the amplitude of the initial film morphology w_0, indicating unstable roughness growth due to film buckling. The viscosity influence is related to the fact that as η decreases, the factor $a(k)$ increases and consequently the contribution of unstable wave vectors $k<h_f^{-1}\sqrt{\beta}$. Indeed, Eq. (5) can be written as

$$w(t)=\left[\frac{(2\pi)^5}{A}\left\{\int_0^{h_f^{-1}\sqrt{\beta}}\langle|h(\mathbf{k},0)|^2\rangle e^{2a(k)t}k\,dk\right.\right.$$
$$\left.\left.+\int_{h_f^{-1}\sqrt{\beta}}^{Q_c}\langle|h(\mathbf{k},0)|^2\rangle e^{2a(k)t}k\,dk\right\}\right]^{1/2}. \qquad (9)$$

The first integral in Eq. (9) yields the contribution of unstable buckling to the film roughness amplitude $w(t)$. Furthermore, with increasing misfit strain ϵ [Fig. 5(b)] the roughness becomes unstable which is characterized by a rapid increment of $w(t)/w_0$. A change of ϵ by 1 order of magnitude leads to a fast transition from a damped buckling behavior [decreasing ratio $w(t)/w_0$] to fast unstable growth of the surface roughness amplitude. This is due to the fact that the range of unstable wave vectors ($k<h_f^{-1}\sqrt{\beta}$) in Eq. (9) becomes larger. It leads to positive values of $a(k)$ and therefore to a faster increase of the roughness amplitude $w(t)$. The effect of the strain ϵ is more pronounced than that of the viscosity η since the former has direct control on the sign of the factor $a(k)$.

Finally, Fig. 6 indicates the influence of the thickness h_f and h_g, respectively, for elastic film and the viscous layer. With decreasing thickness h_f of the elastic film, the minimum or $w(t)$ becomes shallower and a more rapid growth of unstable behavior develops. This is because the range of unstable wave vectors $k<h_f^{-1}\sqrt{\beta}$ increases and consequently the contribution of the first integral in Eq. (9) for $w(t)$. Besides the initial transit regime (up to the minimum), the opposite behavior develops as a function of the viscous film thickness h_g where $w(t)$ increases with increasing viscous thickness h_g.

From the above calculations it becomes clear that in order to determine the limits of film stability as a function of evolution time of buckling, the direct calculation of the surface roughness amplitude is necessary. Although by itself linear stability analysis[4] gives an indication of the stable and unstable wavelengths, it does not provide full knowledge of how these modes contribute as a whole to the buckling roughness amplitude. Note that the film buckling amplitude is a roughness parameter which in real thin film systems can be directly measured, i.e., in terms of scanning probe microscopy[8,9] and x-ray scattering reflectivity.[8,10,11]

V. CONCLUSIONS

We investigated aspects of buckling of compressed elastic thin films, which are bonded onto viscous films of finite thickness. The calculations were limited within the framework of linear elastic plate theory, such that the buckling amplitude remained small in comparison with the film thickness. It was found that the normal stress exerted by the viscous layer on the elastic film evolves with time. It shows a minimum at early buckling stages, while it increases at later buckling stages. Moreover, with decreasing viscosity of the underlying viscous film, the temporal evolution of the film buckling amplitude also shows a minimum. The effect of the viscosity becomes more pronounced with increasing strain in the film. The normal stress also shows a minimum as a function of applied compressive stress with position and shape, which strongly depends on viscosity and strain values. Finally, the unstable growth of buckling roughness is enhanced with decreasing elastic film thickness and/or increasing viscous layer thickness.

ACKNOWLEDGMENTS

The authors would like to acknowledge support from the ''Nederlandse Organisatie voor Wetenschappelijk Onderzoek (NWO)''. They would like also to acknowledge fruitful discussions with Professor E. van der Giessen on the topic of mechanical buckling.

[1] Y. H. Lo, Appl. Phys. Lett. **59**, 2311 (1991).
[2] K. D. Hobart, F. J. Kub, M. Fatemi, M. E. Twigg, P. E. Thompson, T. S. Kuan, and C. K. Inoki, J. Electron. Mater. **2**, 897 (2000).
[3] S. P. Timoshenko and J. M. Gere, Theory of Elastic Solids (McGraw–Hill, New York, 1988).
[4] N. Sridhar, D. J. Srolovitz, and Z. Suo, Appl. Phys. Lett. **78**, 2482 (2001).
[5] W. W. Mullins, J. Appl. Phys. **30**, 77 (1959).
[6] P. Meakin, Phys. Rep. **235**, 199 (1993); P. Meakin, *Fractal, Scaling and Growth Far From Equilibrium* (Cambridge University Press, Cambridge, UK, 1998).
[7] F. Family and T. Viscek, *Dynamics of Fractal Surfaces* (World Scientific, Singapore, 1991).
[8] Y. P. Zhao, G.-C. Wang, and T.-M. Lu, *Characterization of Amorphous and Crystalline Rough Surfaces-Principles and Applications*, Experimental Methods in the Physical Science, Vol. 37 (Academic, New York, 2000).
[9] Y. P. Zhao, G.-C. Wang, and T.-M. Lu, *Characterization of Amorphous and Crystalline Rough Surfaces-Principles and Applications,* Experimental Methods in the Physical Science, Vol. 37 (Academic, New York, 2000).
[10] G. Palasantzas, Phys. Rev. B **48**, 14472 (1993); **49**, 5785 (1994).
[11] S. K. Sinha, E. B. Sirota, S. Garoff, and H. B. Stanley, Phys. Rev. B **38**, 2297 (1988).